

LA-11N-CR  
CAT. 39  
330380  
pdf

**SHEAR BUCKLING OF SPECIALLY ORTHOTROPIC PLATES  
WITH CENTRALLY LOCATED CUTOUTS**

NASA Research Grant NAG-1-917  
Semi Annual Report

February 1991

Eric C. Klang; Principle Investigator

Mechanical and Aerospace Engineering  
North Carolina State University  
Raleigh, NC 27695-7910  
Phone (919) 737 2365

(NASA-CR-187894) SHEAR BUCKLING OF  
SPECIALLY ORTHOTROPIC PLATES WITH CENTRALLY  
LOCATED CUTOUTS Semiannual Report (North  
Carolina Univ.) 20 p CSCL 20K

N91-17429

65/39 Unclas 0330380

## SUMMARY

There is significant industry demand for a method of analyzing the shear buckling of composite plates with cutouts. This method should be able to easily accommodate frequent changes in model design; inflexibility being the major drawback to current finite element methods. The approach taken here is broken into two problems, pre-buckling and buckling. To solve for the pre-buckling stresses, complex variable equations are used in conjunction with boundary collocation. The least squares approach is utilized to improve the accuracy of the results. The buckling problem is solved using the Ritz method. A product of the Ritz method is a complicated integral equation which is solved using numerical integration. To date, the aforementioned method of determining the pre-buckling stresses has been verified against infinite plate theory and finite elements. Recent efforts have focused on reducing run time, improving accuracy and adding more boundary condition choices.

## INTRODUCTION

Laminated composite plates with cutouts are found in many structural applications of aerospace technology. Often structures need cutouts to form access ports for mechanical and electrical systems. Cutouts are also needed in such places as ribs to produce a light airframe. The load carrying capability of plates with cutouts is effected by their pre-buckling and buckling performance, therefore, investigations in this area are essential in designing optimal structural components. The problem of compressive buckling of plates with cutouts has been addressed successfully (ref. 1) , but shear buckling evaluations have been confined to a limited number of specialized finite element analyses (ref. 2). Although finite element analyses produce accurate results, they do not lend themselves to frequent changes in design.

In this summary, a new method for solving the shear buckling problem is introduced. The analysis is based on Lekhnitskii's (ref. 3) complex variable equations, boundary collocation, and the Ritz method. When using finite elements, one must model the entire plate with a large mesh of elements and solve the appropriate equations for each element. Creating the input file which describes the mesh is a tedious and time consuming procedure for the analyst. In applying boundary collocation, it is only necessary to choose points along the plate boundaries at which to solve complex variable equations that describe the applied forces and displacements. By eliminating the need for a complex mesh structure, both manpower time and computer time are reduced. The body of this summary describes in depth the procedure used to analyze the shear buckling problem and gives results which are verified through finite element analyses.

## ANALYSIS

The assumptions made in the analysis presented here are as follows. The x,y coordinate system is located at the center of the plate with the x-axis oriented horizontally. the plate is constructed of a specially orthotropic material. Each edge of the plate can be described as either simply supported or clamped. The cutout is centrally located, is in the form of an ellipse or rectangle, and can be rotated at a given angle from the x-axis. It is possible to load the plate in compression, tension, shear, or any combination of the three, but the main emphasis is on shear loading. The load can be implemented using an applied force or an applied displacement. To solve the problem, the analysis is broken into two separate problems, pre-buckling and buckling.

### Prebuckling Analysis

The pre-buckling part of this analysis is based on Lekhnitskii's (ref. 3) complex variable equations. For a two dimensional stress analysis, the equilibrium equations are:

$$\frac{\partial \sigma_{xx}}{\partial x} + \frac{\partial \tau_{xy}}{\partial y} = 0$$

(1)

$$\frac{\partial \sigma_{yy}}{\partial y} + \frac{\partial \tau_{xy}}{\partial x} = 0$$

The solutions for the stresses in terms of a function F (Airy stress function) are:  
(2)

$$\sigma_{xx} = \frac{\partial^2 F}{\partial y^2} \quad \sigma_{yy} = \frac{\partial^2 F}{\partial x^2} \quad \tau_{xy} = -\frac{\partial^2 F}{\partial x \partial y}$$

Writing the generalized biharmonic equation in terms of F gives:

$$(3) \quad \frac{1}{E_x} \frac{\partial^4 F}{\partial y^4} - \left( \frac{2\nu_{xy}}{E_x} - \frac{1}{G_{xy}} \right) \frac{\partial^4 F}{\partial y^2 \partial x^2} + \frac{1}{E_y} \frac{\partial^4 F}{\partial x^4} = 0$$

Defining:

$$(4) \quad \begin{aligned} z_1 &= x + \mu_1 y & z_2 &= x + \mu_2 y \\ \frac{\partial}{\partial z} &= \frac{\partial}{\partial y} - \mu_k \frac{\partial}{\partial x} & k &= 1, 2 \end{aligned}$$

where  $\mu_k$  are the roots of the characteristic equation:

$$(5) \quad \mu^4 + \left( \frac{E_x}{G_{xy}} - 2\nu_{xy} \right) \mu^2 + \frac{E_x}{E_y} = 0$$

The generalized biharmonic equation can be represented as:

(6)

$$\frac{\partial}{\partial z_1} \frac{\partial}{\partial z_2} \frac{\partial}{\partial z_1} \frac{\partial}{\partial z_2} F = 0$$

the solution for F being:

(7)

$$F = \phi_1(z_1) + \phi_2(z_2) + \phi_1(z_1) + \phi_2(z_2)$$

Substituting F into the stress equations and letting  $\Phi_k(z_k) = \partial \phi_k / \partial z_k$  gives:

(8)

$$\begin{aligned} \sigma_x &= \frac{\partial^2 F}{\partial y^2} = 2^* \text{Re} (\mu_1^2 \Phi_1' + \mu_2^2 \Phi_2') \\ \sigma_y &= \frac{\partial^2 F}{\partial x^2} = 2^* \text{Re} (\Phi_1' + \Phi_2') \end{aligned}$$

$$\tau_{xy} = -\frac{\partial^2 F}{\partial x \partial y} = -2 \operatorname{Re} (\mu_1 \Phi_1' + \mu_2 \Phi_2')$$

Two force equations can be written as:  
(9)

$$2 \operatorname{Re} [\Phi_1(z_1) + \Phi_2(z_2)] \Big|_{\xi_0}^{\xi} = \pm \left( -\int_0^s Y_n ds \right)$$

$$2 \operatorname{Re} [\mu_1 \Phi_1(z_1) + \mu_2 \Phi_2(z_2)] \Big|_{\xi_0}^{\xi} = \pm \int_0^s X_n ds$$

where the upper sign applies to external contours, the lower sign applies to internal contours, and  $s$  is the arclength of a segment on the boundary originating at  $\xi$  and ending at  $\xi_0$ .  $X_n$  and  $Y_n$  are the forces applied to the boundary in the  $x$  and  $y$  directions respectively.

Two displacement equations can be written as:  
(10)

$$2 \operatorname{Re} \left[ p_1 \Phi_1(z_1) + p_2 \Phi_2(z_2) \right] = u$$

$$2 \operatorname{Re} \left[ q_1 \Phi_1(z_1) + q_2 \Phi_2(z_2) \right] = v$$

where:

$$p_k = \frac{1}{E_x} \mu_k - \frac{v_{xy}}{E_x} \quad q_k = \frac{v_{xy}}{E_x} \mu_k + \frac{1}{E_y} \mu_k$$

and  $u$  and  $v$  are the applied displacements in the  $x$  and  $y$  directions respectively. For this analysis, a Laurent series of  $2N+1$  terms will be assumed as follows:  
(11)

$$\Phi_k(z_k) = \sum_{-N}^N A_{kn} z_k^n$$

where  $A_{kn}$  is a complex number,  $c_{kn} + id_{kn}$ .

Substituting the Laurent series representation into the force equation and evaluating from  $i$  to  $i-1$  gives:  
(12 & 13)

$$\begin{aligned}
& 2*\text{Re} \left[ \sum_{-N}^N \{ (c_{1n} + i d_{1n})(z_{1i}^n - z_{1(i-1)}^n) + (c_{2n} + i d_{2n})(z_{2i}^n - z_{2(i-1)}^n) \} \right] = \pm (-Y_n S) \\
& 2*\text{Re} \left[ \sum_{-N}^N \{ \mu_1 (c_{1n} + i d_{1n})(z_{1i}^n - z_{1(i-1)}^n) + \mu_2 (c_{2n} + i d_{2n})(z_{2i}^n - z_{2(i-1)}^n) \} \right] = \pm X_n S
\end{aligned}
\tag{14}$$

Multiplying out the left hand side of equation (12) and finding the real part of the expressing gives:

$$\begin{aligned}
& \sum_{-N}^N \{ c_{1n}(2*\text{Re}(z_{1i}^n - z_{1(i-1)}^n)) + d_{1n}(-2*\text{Im}(z_{1i}^n - z_{1(i-1)}^n)) + \\
& \quad c_{2n}(2*\text{Re}(z_{2i}^n - z_{2(i-1)}^n)) + d_{2n}(-2*\text{Im}(z_{2i}^n - z_{2(i-1)}^n)) \} = \pm (-Y_n S)
\end{aligned}
\tag{15}$$

Similarly for equation (13):

$$\begin{aligned}
& \sum_{-N}^N \{ c_{1n}(2*\text{Re}(\mu_1(z_{1i}^n - z_{1(i-1)}^n))) + d_{1n}(-2*\text{Im}(\mu_1(z_{1i}^n - z_{1(i-1)}^n))) + \\
& \quad c_{2n}(2*\text{Re}(\mu_2(z_{2i}^n - z_{2(i-1)}^n))) + d_{2n}(-2*\text{Im}(\mu_2(z_{2i}^n - z_{2(i-1)}^n))) \} = \pm X_n S
\end{aligned}
\tag{16}$$

The same procedure can be followed for the displacement boundary equations.

For  $n=0$ ,  $(z_{1i})^0 - (z_{1(i-1)})^0 = 1 - 1 = 0$  and the same for  $z_2$ , therefore the coefficients A10 and A20 are arbitrary, thus the Laurent series for becomes:

$$\Phi_k(z_k) = \sum_{-N}^{-1} A_{kn} z_k^n + \sum_1^N A_{kn} z_k^n$$

Solving the force boundary conditions or the displacement boundary conditions around the internal and external boundaries of the plate results in a system of equations which can be arranged in matrix form as follows:

$$[ C_{mkn} ] \{ A_{kn} \} = \{ F_m \}$$

where the  $A_{kn}$  are the unknown Laurent series constants,  $C_{mkn}$  contains the coefficients of the Laurent series constants, and  $F_m$  are the resultant applied forces or applied displacements. To improve the solution of this system of equations, a least squares approach is taken. Using this method, twice as many equations will be used as there are unknowns. Therefore:

[  $C_{mkn}$  ] is a  $16*N \times 8*N$  matrix

$\{ A_{kn} \}$  is a 8\*N vector  
 $\{ F_m \}$  is a 16\*N vector

To solve this system, each side of the system is multiplied by  $[ C_{mkn} ]^T$  as follows:

$$[ C_{mkn} ]^T [ C_{mkn} ] \{ A_{kn} \} = [ C_{mkn} ]^T \{ F_m \}$$

Now there are an equal number of equations and unknowns and the system can be solved directly for the unknown constants. Once the Laurent series constants are calculated, the stress equations (8) can be solved at any given point on the plate.

### Prebuckling Results

A computer program was written to calculate the pre-buckling stresses in a plate with a cutout. The preliminary results were first compared with infinite plate theory. The comparison was made by looking at the shear stress along the x-axis from the edge of a circular cutout to the edge of the plate. At the edge of the hole, the shear stress should equal zero, and at the plate edge, the shear stress should equal the value of the applied load. As the hole size decreases, the complex variable solution should converge to the infinite plate solution. Figure 1 shows the stress distribution for a square plate with a hole radius that is 15% of the plate width. A 100 lb shear stress is applied to the edges of the plate. Figure 2 shows the same plate size and loading conditions with a hole radius that is only 5% of the plate width. For the case of the smaller radius, the infinite solution and the complex variable solution are much closer in value than for the larger cutout. This indicates the expected convergence of the complex variable solution to the infinite plate solution.

To examine the effect of truncating the number of terms in the Laurent series expansion, a comparison was made with finite elements as exhibited in figure 3. In figure 3, the net section shear stress is shown as in figures 1 and 2. The hole radius in this example is 15% of the plate width. The number of terms in the truncated Laurent series is 2\*N. As N increases, the net section stress, as approximated by the complex variable method, approaches the finite element solution. Several contour plots of the stress distribution in plates of varying geometries and material properties were also compared with finite element results and indicated good agreement.

Figures 4 and 5 exhibit the most important advantage of the complex variable method over finite elements. Figure 4 is a contour plot of the shear stress in a rectangular plate with a circular cutout. The length to width ratio of the plate is 2, and the hole radius is 15% of the plate width. The ply layout is [0]24. By changing four lines in the input file, the situation shown in figure 5 can be created and analyzed. Figure 5 shows the shear stress distribution in a square plate with an elliptical cutout rotated 45° to the x-axis. The ply layout here is [(0/90/+45/-45)3]s. In order for finite elements to accommodate these same changes, two separate meshes of several hundred elements would have to be created by the analyst. This procedure would take considerably more time than changing 4 lines of input.

### Buckling Analysis

The determination of the buckling load is based on the Ritz energy method (ref. 4). The strain energy of a structure is represented by:

$$\Pi = U_{is} + U_b \quad (17)$$

where:  
(18 & 19)

$$U_{is} = \frac{1}{2} \iint_A \left\{ \lambda \left[ N_x^0 \left( \frac{\partial w}{\partial x} \right)^2 + N_y^0 \left( \frac{\partial w}{\partial y} \right)^2 + 2 N_{xy}^0 \left( \frac{\partial w}{\partial x} \right) \left( \frac{\partial w}{\partial y} \right) \right] \right\} dA$$

$$U_b = \frac{1}{2} \iint_A \left\{ D_{11} \left( \frac{\partial^2 w}{\partial x^2} \right)^2 + 2 D_{12} \left( \frac{\partial^2 w}{\partial x^2} \right) \left( \frac{\partial^2 w}{\partial y^2} \right) + 4 D_{66} \left( \frac{\partial^2 w}{\partial x \partial y} \right)^2 + D_{22} \left( \frac{\partial^2 w}{\partial y^2} \right)^2 \right\} dA$$

$U_{is}$  is the energy due to the initial stress in the system and  $U_b$  is the energy due to bending.

To solve the strain energy equation, assume the out of plane displacement function,  $w$ , to represent the buckle mode of the plate:

$$w(x,y) = \sum_{m=1}^M \sum_{n=1}^N W_{mn} f_m(x) g_n(y) \quad (20)$$

The displacement function is chosen according to the boundary conditions. Due to the shear loading on the plate, these displacement functions must contain symmetric and antisymmetric modes. For a simply supported plate:

$$w(x,y) = \sum_{m=1}^M \sum_{n=1}^N W_{mn} \sin(m\pi x/a) \sin(n\pi y/b) \quad (21)$$

For a clamped plate:

$$w(x,y) = \sum_{m=1}^M \sum_{n=1}^N W_{mn} [\cos\{(m-1)\pi x/a\} - \cos\{(m+1)\pi x/a\}]^* [\cos\{(n-1)\pi y/b\} - \cos\{(n+1)\pi y/b\}] \quad (22)$$

The total energy of the system is stationary, therefore:

$$\frac{\partial \Pi}{\partial W_{mn}} = 0 \quad (23)$$

Therefore:

$$(24) \quad \sum_{m=1}^M \sum_{n=1}^N \iint_A \{ [D_{11} f''_{m1} f''_{nj} g_n + D_{12} f''_{m1} f''_{nj} g_j g_n + f''_{m1} f''_{nj} g_n] \\ + D_{22} f''_{m1} f''_{nj} g_n + 4D_{66} f''_{m1} f''_{nj} g_j g_n + \\ \lambda N_x^0 f'_{m1} f'_{nj} g_j g_n + \lambda N_y^0 f'_{m1} f'_{nj} g_j g_n + \\ \lambda N_{xy}^0 [f'_{m1} f'_{nj} g_j g_n + f'_{m1} f'_{nj} g_j g_n] \} dA ] W_{mn} = 0$$

The form of the displacement function coupled with the complicated form of the pre-buckling stress equation makes integrating the energy equation extremely difficult, therefore, numerical integration was used. The resulting system of equations constitutes an eigen value problem. Solving for the lowest eigen value gave the critical buckling load of the system.

## BUCKLING RESULTS

Using a Fortran computer code that was written based on the analysis presented herein, buckling loads were calculated for several different square plates with circular cutouts. Cutout diameter to width ratios considered were 0.1, 0.2, 0.3, and 0.4. The plate was made of graphite/epoxy, and several different ply layouts were examined. For the buckling analysis, the plate was considered to be simply supported, and it was loaded in shear through an applied force.

Figure 6 shows the buckling loads for a [(0/90/45/-45)]<sub>3</sub> laminate as obtained from the method presented herein, which will be referred to as the 'complex variable method'. These results are compared with buckling loads acquired from finite element theory. The results shown in figure 6 indicate good agreement at D/W = 0.1, 0.3 and 0.4 where the integration schemes give their most accurate performance. More accuracy in integration was necessary for D/W = 0.2, but could not be achieved due to the large amount of computer time involved.

Figure 7 shows the comparison between the shear buckling loads of finite elements and complex variable theory for a [(45/-45)]<sub>6</sub> laminate.

The buckling loads calculated by the complex variable method show good agreement with finite element theory for all cutout sizes. A comparison of figures 6 and 7 shows that the [(45/-45)]<sub>6</sub> laminate has higher buckling loads under shear loading than does the [(0/90/45/-45)]<sub>3</sub> laminate. The superior performance of the [(45/-45)]<sub>6</sub> laminate is attributed to the fact that the fibers in the laminate are aligned in the direction of the acting forces.

The buckling loads of a [(60/-60)]<sub>6</sub> (or [(30/-30)]<sub>6</sub>) laminate are shown in fig. 8. There is good agreement between finite elements and complex variable theory for D/W = 0.1 and 0.3, but the buckling loads for D/W = 0.2 and 0.4 are not calculated as well. Again, computer time was a factor in that error margins could not be decreased to a desired level without extensive usage of computer time. A comparison of figures 7 and 8 shows that, as the fiber angle rotates away from the lines along which the forces act, the buckling loads decrease as does the accuracy of the complex variable solution.

Figure 9 is a plot of the buckling loads for a [(15/-15)]<sub>6</sub> (or [(75/-75)]<sub>6</sub>) laminate under shear loading. Once again, as the fiber angle is rotated farther away from the force direction, the buckling loads decrease, as well as the accuracy of the complex variable method.

## INTEGRATION TECHNIQUES

It was felt that the accuracy of the solution was strongly dependant on the integration scheme used to integrate equation 24. The final effort of this work therefore centered on improving this portion of the computational scheme.

The first attempt at improving the integration involved the closed form integration of the terms in equation 24 which did not contain the pre-buckling stresses. This was successfully accomplished when it was decided to include the possibility of new boundary conditions (other than simply supported and clamped). This meant that the assumed form of the out-of-plane displacement would be different and hence the integration of equation 24 would be altered. The displacement functional used was a modified form of that chosen for the beam analysis of Razzaq et. al. [5]. This displacement functional allowed the boundary conditions to range from simply supported to clamped by including rotational stiffness along the edge. The grant ended just as these new improvements were being added to the code.

## CONCLUDING REMARKS

Lekhnitskii's complex variable equations were used with boundary collocation to determine the pre-buckling stresses of composite plates with centrally located cutouts loaded in shear. This method was in good agreement with infinite plate theory and finite element solutions. The extremely small input files necessary to instruct the complex variable program, as opposed to the lengthy finite element mesh files, saves significant manpower time. The easy adaptation of the method proposed herein to several plate and cutout geometries allows for frequent structural design changes and is appropriate for parametric studies.

The Ritz energy method was chosen to analyze the buckling problem. An out of plane displacement function was assumed according to the boundary conditions. The complicated form of the out of plane displacement function and the pre-buckling stress equation led to the use of numerical integration to simplify the energy equation. The resulting system of equations constituted an eigen value problem which was solved for the buckling loads. Preliminary results using a low number of waves in the displacement function gave reasonable results, but a higher number of waves will be necessary to achieve accurate results.

The attempts at improving the accuracy of the solution by finding closed form solutions for some of the integrals was showing good promise when the grant was terminated.

## REFERENCES

1. Nemeth, Micheal P.: A Buckling Analysis for Rectangular Orthotropic Plates with Centrally Located Cutouts, NASA Technical Memorandum 86263, December, 1984.
2. Sabir, A. B. and Chow, F. Y.: Elastic Buckling of Flat Panels Containing Circular and Square Holes, Proceedings of The Micheal R. Horne Conference.
3. Lekhnitshii, S. G.: Theory of Elasticity of an Anisotropic Body, MIR Publishers, Moscow, 1981.

4. Whitney, James M.: Structural Analysis of Laminated Anisotropic Plates, Technomic Publishing Co., Lancaster, Pennsylvania, 1987.
5. Razzaq, Zia; Volland, R. T.; Bush, H. G. and Mikulas, M. M. Jr.: *Stability, Vibration, and Passive Damping of Partially Restrained Imperfect Columns*, NASA Technical Memorandum 85697, October 1983.

**Net-Section Shear Stress for a Square Plate with 15% Hole**

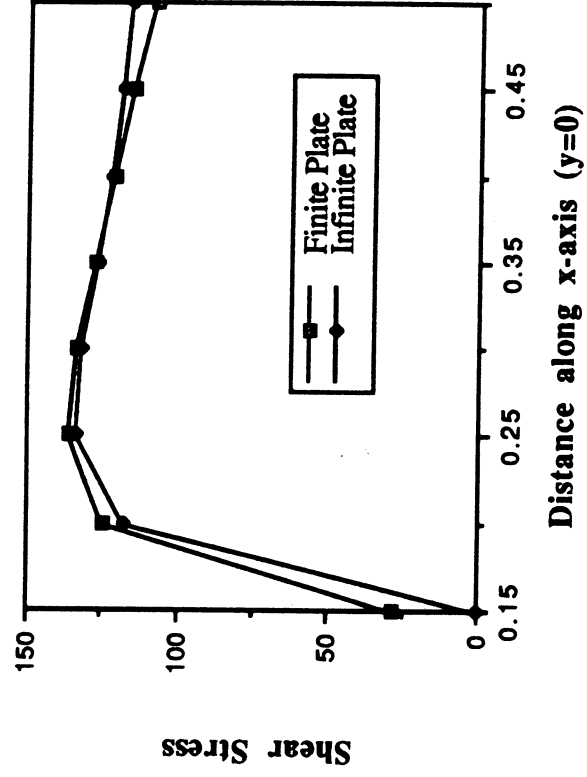


**Figure 1**

**Net-Section Shear Stress for a Square Plate with 5% Hole**

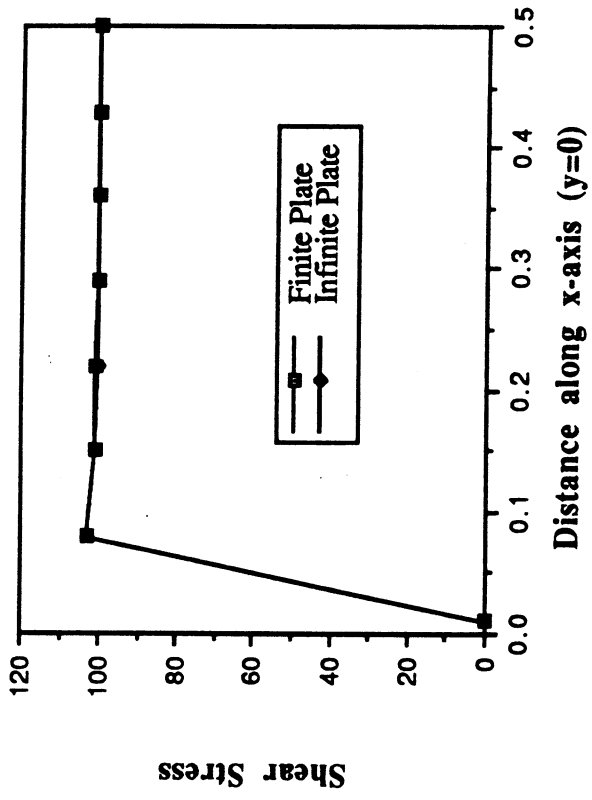


**Figure 2**

**Comparison of Net-Section Shear Stresses with Finite Element Results**

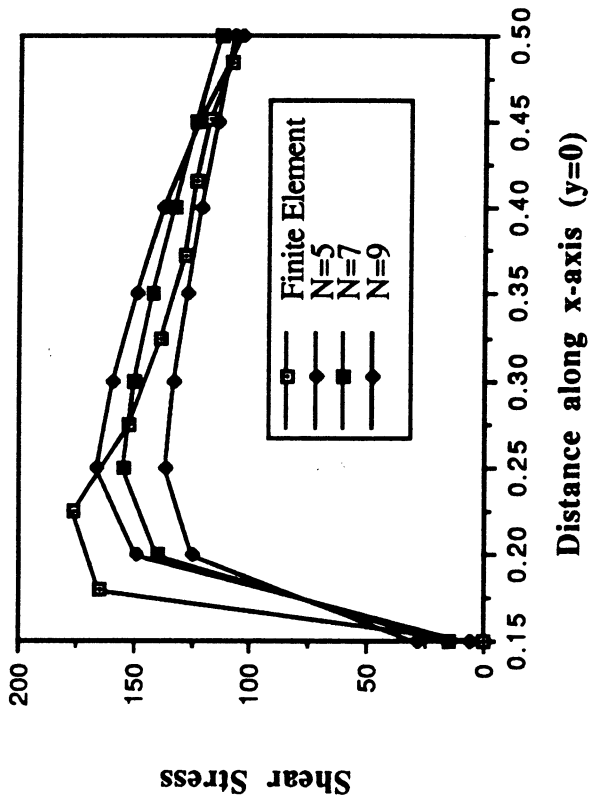


**Figure 3**

**Shear Stress Contours For a Rectangular Plate with a Circular Cutout**

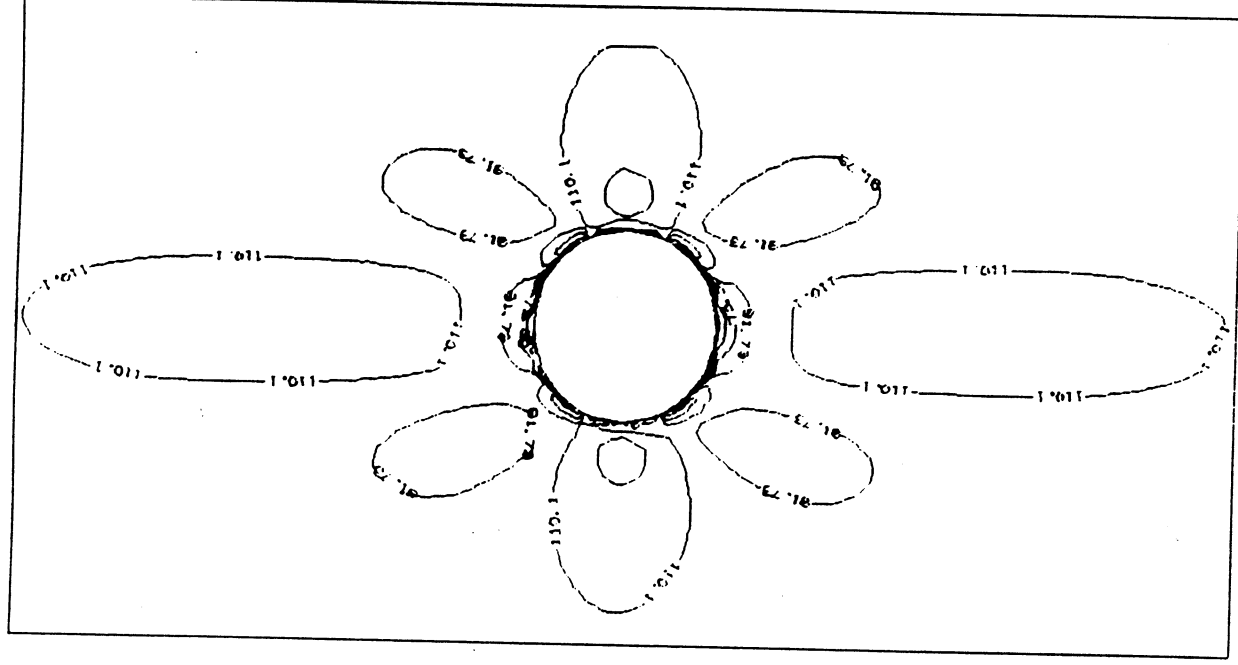


**Figure 4**

**ORIGINAL PAGE IS  
OF POOR QUALITY**

**Shear Stress Contours For a Square Plate with a Rotated Elliptical Cutout**

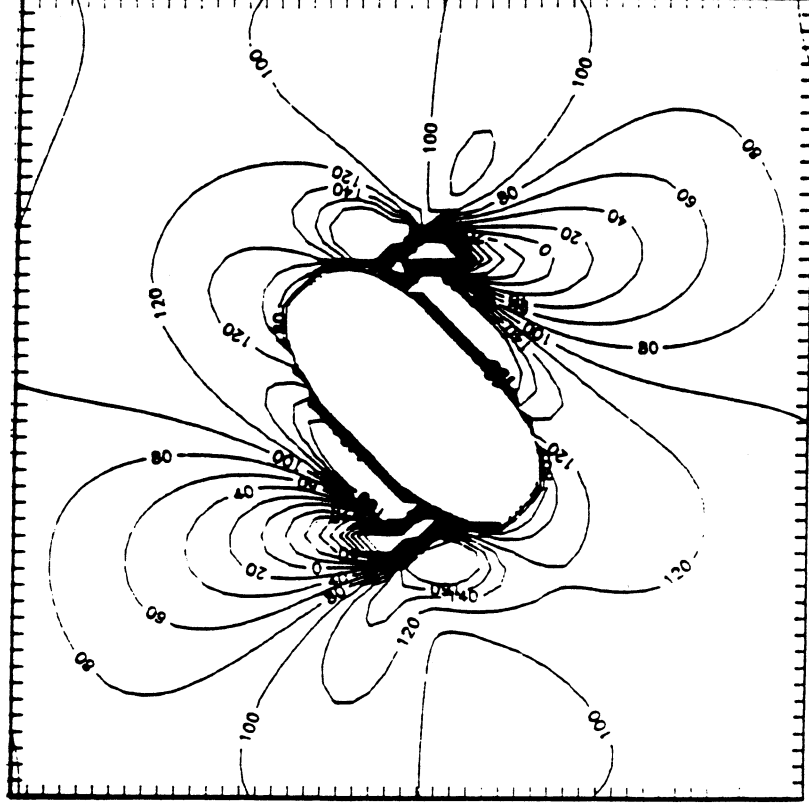


**Figure 5**

Buckling Loads ((0/90/45/-45)<sub>3</sub>IS)

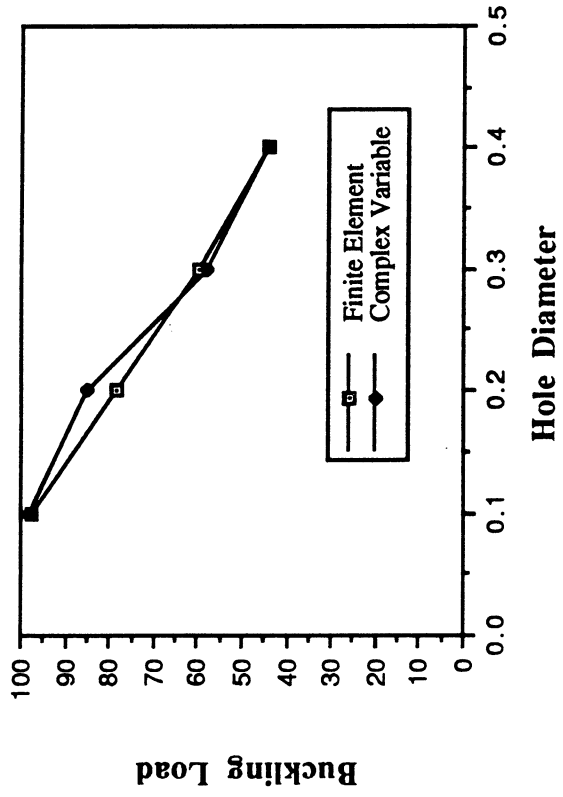


Figure 6

Buckling Loads ( $[(45/-45)6]S$ )

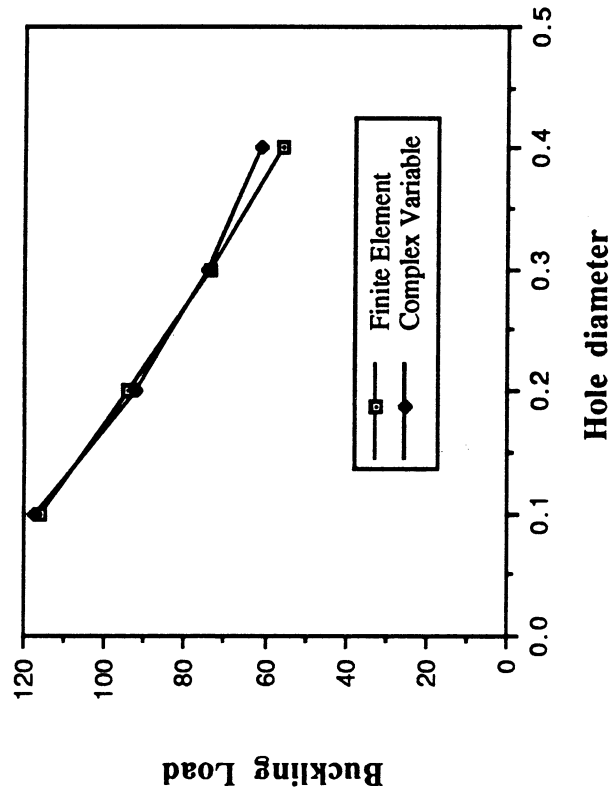


Figure 7

Buckling Loads ([(60/-60)]s or [(30/-30)]s)

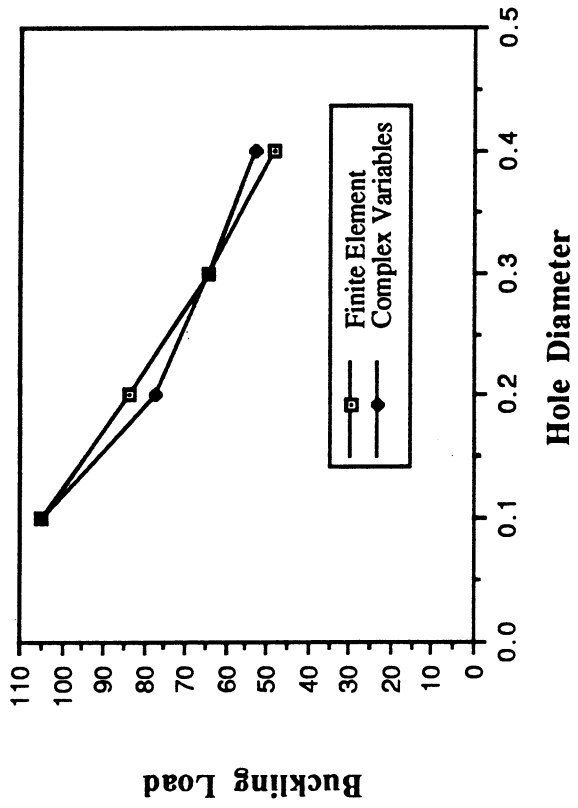


Figure 8

Buckling Loads ((15/-15) or (75/-75))

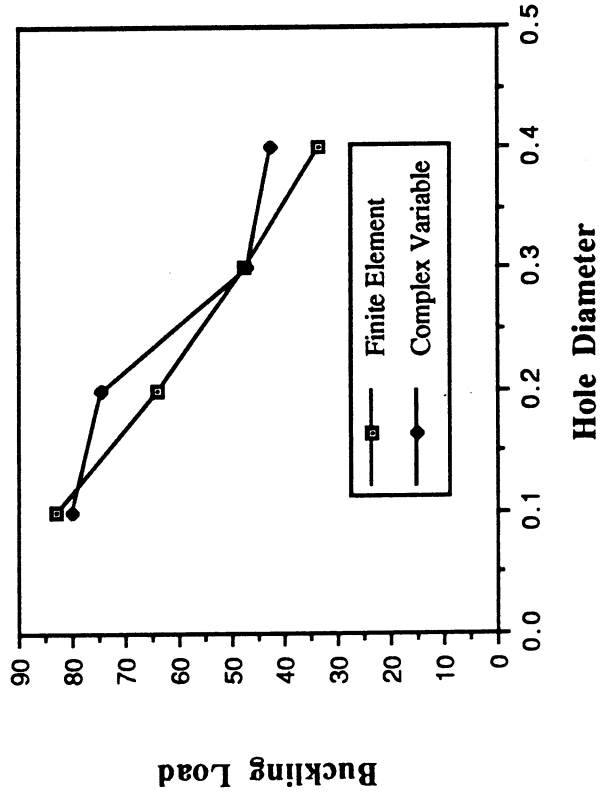


Figure 9